11

Polyoxometalate Nanocapsules: from Structure to Function

Charalampos Moiras and Leroy Cronin

11.1
Introduction

The assembly of nanoscale capsules or cages using metal coordination represents one of the most interesting and challenging areas of chemical nanoscience today. This is because these capsules are composed of many discrete metal- and ligand-based building blocks which have the ability to self-assemble into a single gigantic [1], even protein-sized [2], species, often rapidly and in high yield; most of these have very high symmetry [3], rendering them aesthetically extremely appealing. However, the interest in these systems goes far beyond aesthetics since understanding of the principles and mechanism for the assembly process which leads to their formation will allow systems to be designed from first principles. In this chapter we discuss how polyoxometalate-based molecular capsules and cages are defining a new class of capsules and nanospaces [4]. Nanoscale polyoxometalate clusters (POMs) provide an arguably unrivalled structural diversity of molecules displaying a wide range of important physical properties and nuclearities; these cover the range from 6 to 368 metal ions in a single molecule and are assembled under "one-pot" reaction conditions. At the extreme, these cluster molecules are truly macromolecular, rivaling the size of proteins, and are thought to be formed by a self-assembly process (Figure 11.1) [5]. The clusters are based on metal–oxide building blocks with the general formula MO_x (where M is Mo, W, V and sometimes Nb and x can be 4, 5, 6 or 7). POM-based materials have many interesting physical properties which result from their versatile structures, the ability to delocalize electrons over the surface of the clusters, the ability to incorporate heteroanions, electrophiles and ligands and to encapsulate guest molecules within a metal–oxide-based cage. POM clusters have been shown to exhibit superacidity and catalytic activity [6], photochemical activity [7], ionic conductivity [7] and reversible redox behavior [8]. Therefore, there are many potential applications for this class of molecules [4–8].
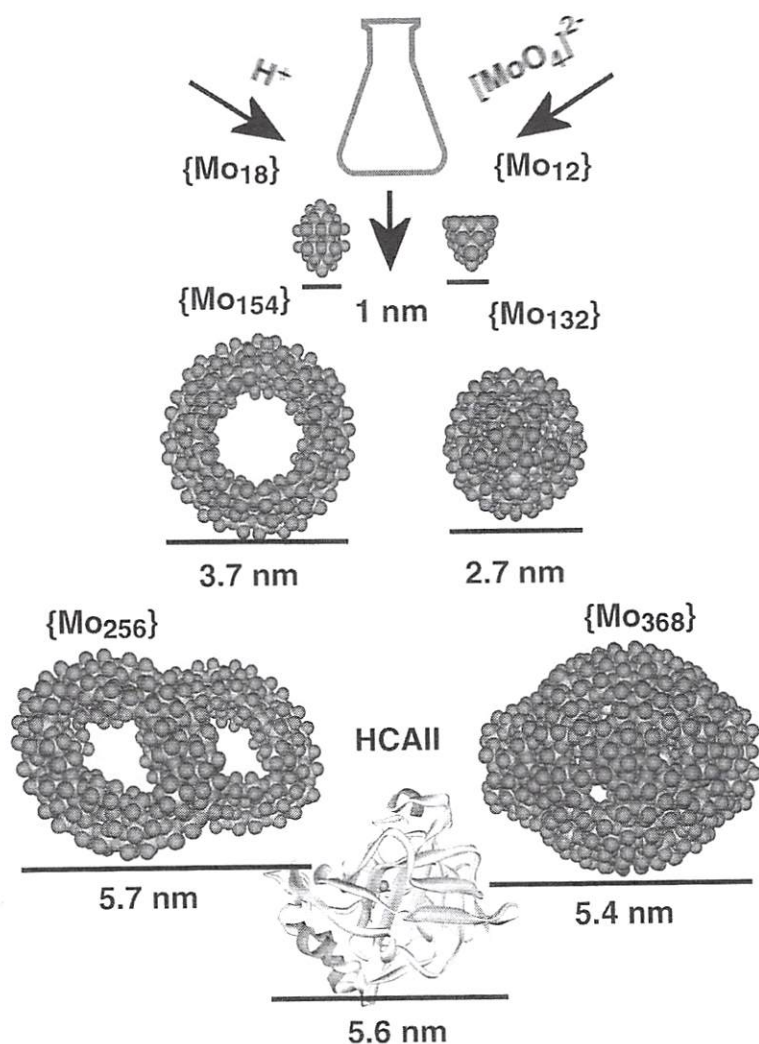
Figure 11.1 Representations of the structures of some POM clusters, all synthesized under "one-pot–one-step" reaction conditions (space filling: Mo large gray spheres, O smaller gray spheres) from the well-known and studied $\{M_{12}\}/\{M_{18}\}$ Keggin–Dawson ions to the $\{Mo_{154}\}/\{Mo_{132}\}$ and $\{Mo_{256}\}/\{Mo_{368}\}$ clusters. These clusters are compared (to scale) with the protein human carbonic anhydrase II (a medium-sized protein with 260 residues, MW 29.6 kDa) to demonstrate their macro dimensions.

Importantly, the assembly of coordination cages involving metal ligand coordination to mediate the self-assembly process depends critically on the building blocks chosen and their respective reactivities. One very important route to the formation of metallosupramolecular architectures involves the selection of building blocks that (1) are preorganized, (2) are kinetically stable, (3) incorporate reactive coordination sites and (4) are complementary. For instance, the exhaustive

study of the molybdenum, tungsten and vanadium oxide systems, i.e. polyoxometalate clusters, has emerged as one of very important and versatile building block source in molecular self-assembly [4,5].

11.2
Background and Classes of Polyoxometalates

The large number of structural types in polyoxometalate chemistry [4,5] can be broadly split into three classes:

1. Heteropolyanions are metal–oxide clusters that include heteroanions such as SO_4^{2-} and PO_4^{3-}. These represent by far the most explored subset of POM clusters, with over 5000 papers being reported on these compounds during the last 4 years alone. There is great emphasis on catalysis in this literature, of which the Keggin $[XM_{12}O_{40}]$ and the Wells–Dawson $[X_2M_{18}O_{54}]$ (where M=W or Mo) anions are fundamental examples. Their popularity, reflected in an enormous volume of literature over several decades, can be attributed to a large extent to the ease of their synthesis or commercial availability, but most importantly to the stability of these clusters. In particular W-based POMs are very stable and this has been exploited to develop W-based Keggin ions with vacancies that can be systematically linked using electrophiles to larger aggregates [4,5].

2. Isopolyanions are composed of a metal–oxide framework, but without the internal heteroatom/heteroanion. As a result, they are often much more unstable than their heteropolyanion counterparts. However, they also have interesting physical properties, such as high charges and strongly basic oxygen surfaces, which means that they are attractive units for use as building blocks [9].

3. Mo-blue and Mo-brown reduced Mo-based POM clusters are related to molybdenum blue-type species, which was first reported by Scheele in 1783 [10]. Their composition was largely unknown until Müller et al. reported, in 1995, the synthesis and structural characterization of a very high nuclearity cluster $\{Mo_{154}\}$ crystallized from a solution of Mo-blue, which has a ring topology [11]. The interest generated by this result is partly due to its high nuclearity and partly because of the size of this cluster; with an outer diameter of ca. 34 Å, an inner diameter of 25 Å and a thickness of 14 Å, it is a truly nanoscopic molecule. Using reaction conditions of pH $\approx$ 1, with a concentration of Na_2MoO_4 of ca. 0.5 M and a degree of reduction of between 1 and 20%, the solution yields the "giant-wheel" $[Mo_{154}O_{462}H_{14}(H_2O)_{70}]^{14-}$ in over 80% yield in 24 h [12]. The building up principle does not stop there: a series of mixed-valence Mo-blue (containing delocalized Mo^V–Mo^{VI}) clusters (e.g. $[Mo_{256}Eu_8O_{776}H_{20}(H_2O)_{162}]^{20-} \equiv \{Mo_{256}\}$) [13] have been reported and also a class of spherical Mo-brown (containing localized Mo^V–Mo^V units) clusters (e.g. $[Mo^{VI}_{72}Mo^V_{60}O_{372}(MeCO_2)_{30}(H_2O)_{72}]^{42-} \equiv \{Mo_{132}\}$) [14] and the highest nuclearity cluster so far found, a "lemon" cluster $([H_xMo_{368}O_{1032}(H_2O)_{240}(SO_4)_{48}]^{48-} \equiv \{Mo_{368}\})$ [2] (Figure 11.2).
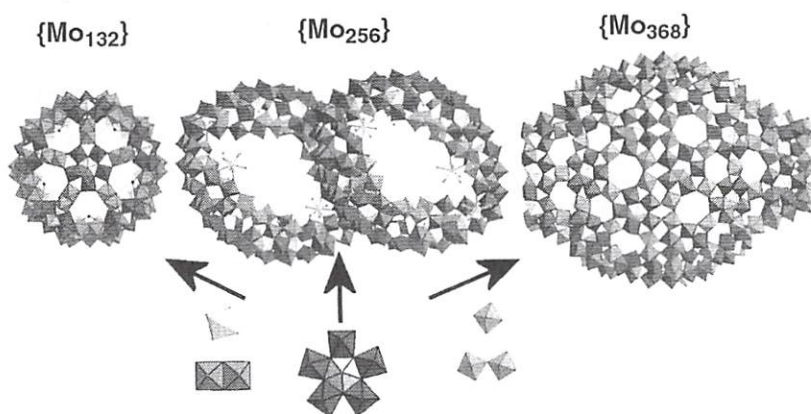
{Mo$_{132}$}   {Mo$_{256}$}   {Mo$_{368}$}

Figure 11.2 Structures of the {Mo$_{132}$} ≡ [Mo$^{VI}_{72}$ Mo$^{V}_{60}$O$_{372}$(MeCO$_2$)$_{30}$(H$_2$O)$_{72}$]$^{42-}$, {Mo$_{256}$} ≡ [Mo$_{256}$Eu$_8$O$_{776}$H$_{20}$(H$_2$O)$_{162}$]$^{20-}$ and {Mo$_{368}$} ≡ [H$_x$Mo$_{368}$O$_{1032}$(H$_2$O)$_{240}$(SO$_4$)$_{48}$]$^{48-}$ clusters shown with polyhedral plots. The transferable building blocks found in these clusters are shown below also as polyhedral plots whereby the metal is at the center of the polyhedron and the oxygen ligands form the vertexes.

11.3
Wells–Dawson {M$_{18}$O$_{54}$} Capsules

The Wells–Dawson cluster type can be considered to be an {M$_{18}$O$_{54}$}$^{m-}$ cluster that often incorporates either one or two templating anionic units e.g. PO$_4^{3-}$ and SO$_4^{2-}$ [5], so the cluster can be formulated as ([M$_{18}$O$_{54}$(XO$_n$)$_2$]$^{m-}$; M=Mo or W, X = a main group element, n = 3 or 4) (Figure 11.3). The {M$_{18}$O$_{54}$}$^{m-}$ can be considered to have a hydrophilic cavity and can incorporate many types of different anions; traditionally these have been either PO$_4^{3-}$ or SO$_4^{2-}$ [4,5]. By incorporating electronically interesting anions such as sulfite, it is possible to engineer several types of cluster cage
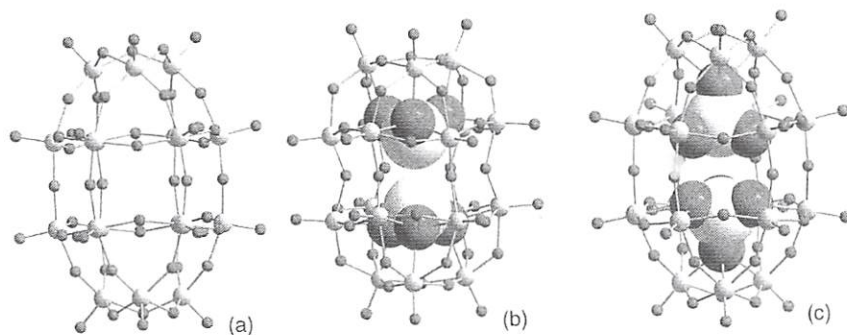

(a)   (b)   (c)

Figure 11.3 Ball and stick representations of (a) {M$_{18}$O$_{54}$}$^{m-}$, (b) [Mo$_{18}$O$_{54}$(SO$_3$)$_2$]$^{4-}$ and (c) [Mo$_{18}$O$_{54}$(SO$_4$)$_2$]$^{4-}$. The M atoms are shown as small gray spheres and the O atoms as dark gray spheres. The S and O atoms of the SO$_3$ and SO$_4$ groups are shown in space filling mode.

whereby the anions can themselves interact with each other or undergo reactions inside the cluster cage. This sulfite-containing cluster can be formulated [15] as $[Mo_{18}O_{54}(SO_3)_2]^{4-}$ and the sulfites as positioned within the cluster cage such that they are located only 3.2 Å apart from each other inside the cluster shell (this is 0.4 Å less than the 3.6 Å expected from non-bonded S···S interactions but still longer than the 2.2 Å found in $S_2O_6^{2-}$) and could indicate a strong interaction between the two sulfur atoms; this was also suggested by DFT calculations [15]. In the limit it was thought that engineering such capsules may allow the oxidation of sulfite to yield dithionate $S_2O_6^{2-}$ anions (note: sulfur is the only main group element to form $X_2O_6^{n-}$ analogues with X—X single bonds), e.g.

$$2SO_3^{2-} \longrightarrow S_2O_6^{2-} + 2e^-$$
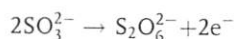
Thus, engineering an intramolecular S···S interaction within the Dawson $\{Mo^{VI}_{18}\}$ matrix is interesting since the formation of a dithionate anion would release two electrons to reduce the surrounding polyoxomolybdate shell to the mixed-valence reduction state $\{Mo^{VI}_{16}Mo^{V}_{2}\}$, with its characteristic blue color. Although switching has not yet been achieved, the sulfite-based clusters are thermochromic between 77 and 500 K [15].

By altering the synthetic conditions, it is also possible to obtain a sulfite-based polyoxotungstate, α-$[W_{18}O_{54}(SO_3)_2]^{4-}$ [16], which is isostructural with α-$[Mo_{18}O_{54}(SO_3)_2]^{4-}$ [14], and $[W^{VI}_{18}O_{56}(SO_3)_2(H_2O)_2]^{8-}$ [16]. The latter is described as a "Trojan horse" in which a structural rearrangement allows the two embedded pyramidal sulfite (SO_3^{2-}) anions to release up to four electrons (analogous to the "soldiers" hidden inside the "Trojan horse") to the surface of the cluster generating the sulfate-based, deep-blue, mixed-valence cluster $[W_{18}O_{54}(SO_4)_2]^{8-}$ upon heating (Figure 11.4). The sulfite anions adopt a radically different orientation in $[W^{VI}_{18}O_{56}(SO_3)_2(H_2O)_2]^{8-}$,

$$[W^{VI}_{18}O_{56}(S^{IV}O_3)_2(H_2O)_2]^{8-} \xrightarrow{\Delta \ ca. \ 400°C} [W^{VI}_{14}W^{V}_4O_{54}(S^{VI}O_4)_2]^{8-} + 2\ H_2O$$
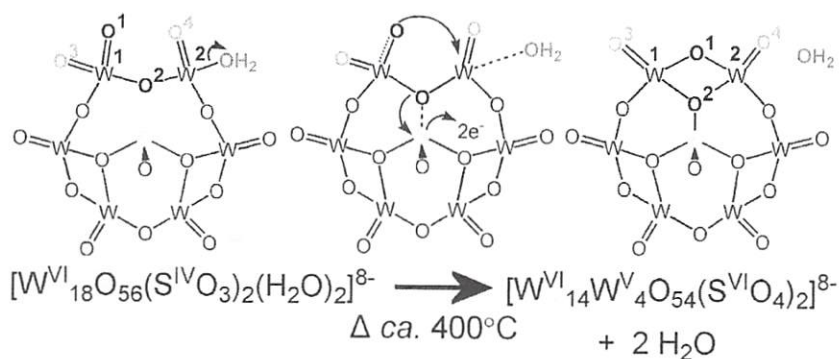
Figure 11.4 Scheme showing the change in the metal oxo framework on one half of the cluster upon oxidation of the internal SO_3^{2-} ligand to SO_4^{2-} (shown by the movement of each of the number oxygen atoms on the left to the end position on the right), which is commensurate with the reduction of the cluster shell by four electrons, giving rise to the deep-blue material from the colorless crystals.

whereby they each only ligate to seven metal centers: three from the cap and four (out of six) from the "belt" of the cluster framework.

The orientation for the sulfite anions within the cluster type is somewhat like the coordination mode for the tetrahedral templates (XO_4^{y-}) in conventional Dawson $[M_{18}O_{54}(XO_4)_2]^{2y-}$, i.e. one of the oxo ligand bridges three capping W centers, and the remaining oxo ligands each bridge two of the "belt" W centers. Nevertheless, this leaves two "belt" W atoms uncoordinated to the template SO_3 moiety as SO_3 has one oxo ligand less than XO_4. Hence it can be seen that the sulfite ions are grafted on to the bottom side of the cluster, which resembles a "basket" with four "uncoordinated" "belt" metal centers on the top part and now has a lower C_{2v} symmetry compared with the cluster α-$[Mo_{18}O_{54}(SO_3)_2]^{4-}$, which has a D_{3h} symmetry. To compensate for the coordination, these unique "uncoordinated" "belt" W centers (four for the whole cluster) each have two terminal ligands, rather than one as found for the remaining metal centers in the cluster. These are in addition to the four other μ_2 bridging oxo (O^{2-}) ligands between metal centers and complete a slightly distorted octahedral coordination geometry for each of the four "uncoordinated" "belt" metal centers concerned. Single-crystal structure analysis revealed that two of the four unique metal centers each have two W=O terminals (W–O $\approx$ 1.7 Å) and the other two each have one W=O terminal and one W–OH$_2$ terminal (W–O $\approx$ 1.7 and 2.2 Å, respectively). Furthermore, it is interesting that the unique "belt" μ_2 bridging oxo ligands between the pair "uncoordinated" "belt" W atoms now bends in towards the cluster, rather than outwards as normal, and is located ca. 2.9 Å distant from the sulfur center of the SO_3 moiety, whereas the two sulfur centers are positioned 3.6 Å apart at opposite sides of the cluster shell. In this respect, the mechanism for the reduction of the cluster shell requires an interaction between the sulfur atom and the special belt oxo ligand, which then react to form two sulfate anions located within the $\{W_{18}\}$ cluster shell.

In summary, compounds $[Mo_{18}O_{54}(SO_3)_2]^{4-}$ and $[W_{18}O_{56}(SO_3)_2(H_2O)_2]^{8-}$ demonstrate unprecedented electronic properties, thermochromism and a unique electron-transfer reaction, in which, when heated, a structural rearrangement allows the two embedded pyramidal sulfite ($S^{IV}O_3^{2-}$) anions to release up to four electrons to the surface of the cluster, generating the sulfate-based, deep-blue, mixed-valence cluster $[W_{18}O_{54}(SO_4)_2]^{8-}$. Although electron-transfer reactions and structural rearrangements are known for HPOMs, these electron transfer reactions are "confined" within a molecular nanocage whereby the electrons are "released" from the core of the cluster. Moreover, this property is really intriguing, from the point of view of nanoscience, and $[W_{18}O_{56}(SO_3)_2(H_2O)_2]^{8-}$ can be considered to be a prototype nanodevice which responds according to a stimulus.

11.4
Isopolyoxometalate Nanoclusters

Going one step further, someone could realize the fact that porosity, separation and ion transportation effects start being a noteworthy feature of the POM capsules.
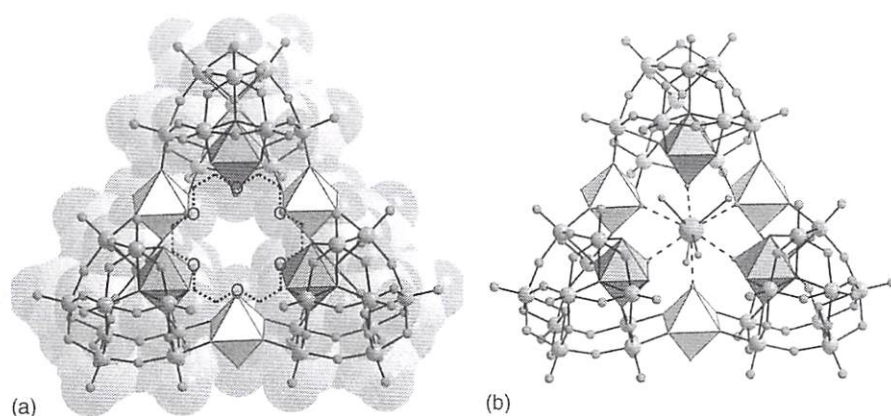
(a)

(b)

Figure 11.5 (a) Comparative illustration of the {W_{36}} cluster framework [$H_{12}W_{36}O_{120}$]$^{12-}$ and the 18-crown-6 structure (show to scale). W and O atoms shown as light and dark spheres, respectively, with the crown ether superimposed on O atoms forming the "cavity" of the cluster. The ball and stick structure is also superimposed on the space-filling CPK representation, along with a polyhedral representation of the six W units that provide the "crown" coordinating O atoms.

(b) The same ball and stick/polyhedral structure but this time showing the complexed potassium ion and the ligated water molecules within the cavity representing the overall {$(H_2O)_4K \subset [H_{12}W_{36}O_{120}]$}$^{11-}$ complex.

The {W_{36}}-based cluster with the formula {$(H_2O)_4K_{[H_{12}}W_{36}O_{120}]$}$^{11-}$ includes the threefold symmetric cluster anion [$H_{12}W_{36}O_{120}$]$^{12-}$ (Figure 11.5) [17]. The cluster anion complexes a potassium ion at the center of the {W_{36}} cluster in an O_6 coordination environment. The {W_{36}} structure consists of three {W_{11}} subunits; these subunits contain a ring of six basal W positions, an additional W position in the center of this ring and four apical W positions in a butterfly configuration. Every W position around the cluster center has a distorted WO_6 octahedral coordination geometry with one terminal W=O moiety [d(W=O) $\approx$ 1.70 Å] extending towards the cluster center where the K ion is located; this arrangement maps extremely well on to the structure of the crown ether [18]crown-6.

The implications for the development of this system in a similar fashion to the crown ethers is interesting, especially the possibilities for discrimination and sensing of metal ions using this cluster framework [18]. The crown ether-like properties for the {W_{36}} cluster can be realized in the presence of other cations such as K$^+$, Rb$^+$, Cs$^+$, NH$_4^+$ and Sr^{2+}, and it was determined that these ions can bind to the cluster and their structures crystallographically determined (Table 11.1).

As can be seen in the table, the found average oxygen–metal distances in the {W_{36}} host–guest complexes 1–5 are very close to the distances shown in the corresponding 18-crown-6 complexes. The metal cations in the synthesized compounds show different distances to the equatorial plane of the cluster framework which reflect the different sizes of their ionic radii. Although there are some great similarities between the {W_{36}} system and 18-crown-6, there are some features that are not common to both systems. First, the six-coordinated oxygen atoms on {W_{36}} are not

Table 11.1 Comparison of acquired metal–oxygen distances and displacements of metal ions to the cavity center in the $\{W_{36}\}$ cluster and the corresponding figures for the 18-crown-6 ether (e.s.d.s are all with 0.02 Å).

Cation	Ionic radius (Å)	Average metal–oxygen distance (Å)		Distance from cavity center (Å)	
		$\{W_{36}\}$ cluster	18-Crown-6	$\{W_{36}\}$ cluster	18-Crown-6
K^+	1.38	2.80	2.80	0.70	0
Rb^+	1.52	2.87	2.95	0.84	0.93
Cs^+	1.67	3.16	3.18	1.61	1.47
Sr^{2+}	1.18	2.70	2.73	0.53	0
Ba^{2+}	1.35	2.82	2.82	0.73	0

planar, whereas those on 18-crown-6 can adopt a planar conformation. Further, the $\{W=O\}_6$ donor groups of the $\{W_{36}\}$ crown are rigid, unlike in 18-crown-6, which is much more flexible. This means that 18-crown-6 can deform to form metal complexes with small ions such as Na^+, Ca^{2+}, lanthanide ions and d-transition metal ions. This is because 18-crown-6, along with other similar crown ethers, is able to distort and wrap itself around these smaller metal cations in an attempt to maximize the electrostatic interactions. This increases the strain of the ligand, which makes these complexes less stable than those with metal cations of optimal spatial fit. However, the $\{W_{36}\}$ framework, due to its high rigidity, simply cannot change conformation in such a way as to bind these metal cations. This is partly confirmed by the observation that the diameter of the central cavity present in the family of $\{W_{36}\}$ clusters presented here is very well defined and rigid.

11.5
Keplerate Clusters

Reduced polyoxomolybdate clusters represent one of the most interesting cluster classes for nanoscience as these clusters adopt ring and spherical shapes comprising pentagonal $\{(Mo)Mo_5\}$ building blocks [5]. In particular, the spherical icosahedral $\{Mo_{132}\}$ Keplerate cluster as been described as an inorganic superfullerene due to its symmetry and large nanoscale size [19]. The discovery of such a cluster, particularly as it is spherical, water soluble and has such a large cavity, probably represents one of the most significant findings in recent years [20], especially since this discovery has gone on to reveal a whole family of related Keplerates. Within this family [20–33], all the spherical and approximately icosahedral clusters have the form $[\{(pent)_{12}(link)_{30}\}]$, e.g. like $[\{(Mo)(Mo_5O_{21}(H_2O)_6\}_{12}\{Mo_2O_4(ligand)\}_{30}]^{n-}$ with binuclear linkers where the 12 central pentagonal units span an icosahedron and the linkers form a distorted truncated icosahedron; the highly charged capsule with sulfate ligands and $n = 72$ was used very successfully. For instance, the truly nanoscale capsules (inner cavity diameter ca. 2.5 nm) allow different types of encapsulations, e.g. of well-structured
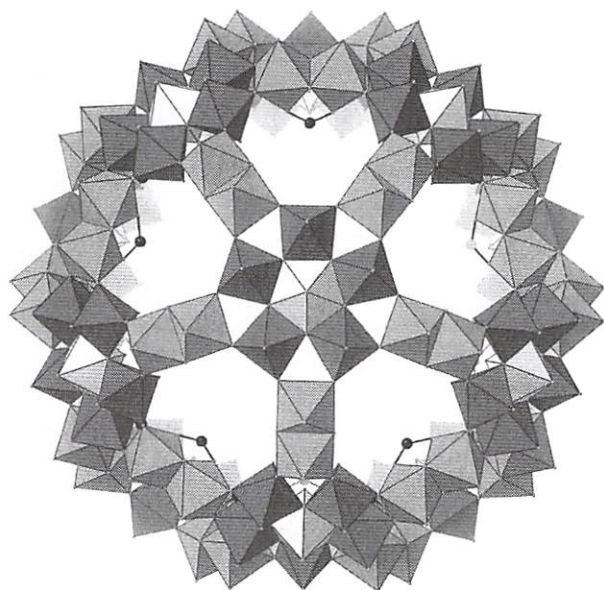
Figure 11.6 A polyhedral representation of the $\{Mo_{132}\}$ Keplerate cluster. The pentagonal $\{Mo_6\}$ building blocks and the $\{Mo_2\}$ building blocks can be seen. The bridgehead atom of the XO_2 bridge of the $\{Mo_2\}$ groups can be seen as black spheres.

large water assemblies (up to 100 molecules) with an "onion"-like layer structure enforced by the outer shell (Figure 11.6) [21]. Most importantly, the capsules have 20 well-defined pores and the internal shell functionalities can be tuned precisely since the nature of the bidentate ligands can be varied. In the special case of binuclear $Mo^V_2O_4{}^{2+}$ linkers the pores are $\{Mo_9O_9\}$ rings with a crown ether function (diameters 0.6–0.8 nm) which can be reversibly closed, e.g. by guanidinium cations interacting noncovalently with the rings via formation of hydrogen bonds [22]. In a related smaller capsule with mononuclear linkers, the $\{Mo_6O_6\}$ pores can become closed/complexed correspondingly by smaller potassium ions [23].

The most intriguing and exciting property of the highly negatively charged capsules is that they can mediate cation transfer from the solution to the inner nanocavity. Indeed, reaction of the above-mentioned highly charged capsule with different substrates/cations such as Na^+, Cs^+, Ce^{3+}, $C(NH_2)_3{}^+$ and $OC(NH_2)NH_3{}^+$ in aqueous solution leads to formations/assemblies which exhibit well-defined cation separations *at*, *above* or *below* the capsules channel-landscapes ("nano-ion chromatograph" behavior) [24]. Taking this one step further, a temperature-dependent equilibrium process that involves the uptake/release of Li^+ ions through the capsule pores has been observed: the porous capsule behaves as a semipermeable inorganic membrane open for H_2O and small cations [25,26]. Furthermore, the 20 pores of the same capsule "shut" by protonated urea as "stoppers" can be opened in solution, thus allowing calcium(II) ion uptake while later closing occurs again (Figure 11.7) [27]. Remarkably,
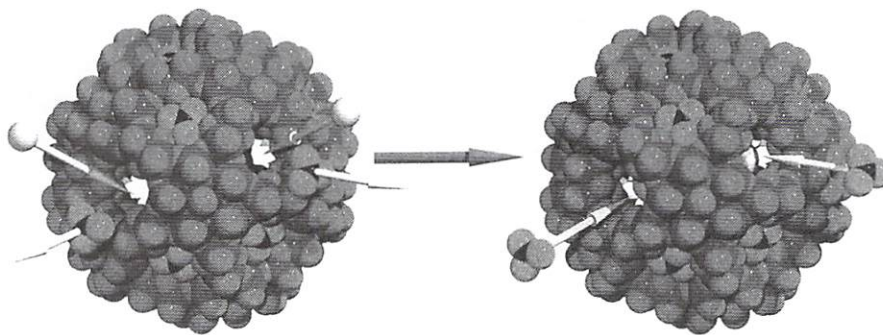
Figure 11.7 Space-filling representation demonstrating a simplified view of the Ca^{2+} ion uptake based on the capsule $[\{(Mo)(Mo_5O_{21}(H_2O)_6\}_{12}\{Mo_2O_4(SO_4)\}_{30}]^{72-}$. Initially the pores are closed, but treating a solution of the capsule with Ca^{2+} ions leads to cation uptake (left) while in the final product the pores again are closed (right; Mo, dark gray, O, medium gray, C, black, N/O(urea), light gray, Ca^{2+}, light gray spheres).

"pore gating" – just modeling biological ion transport – can illustratively be demonstrated: after initial cation uptake, subsequent cations are found hydrated above the pores due to a decrease of negative capsule charge [28].

This type of nanocapsules proved their efficiency in cation separation processes also in the presence of heavier metal atoms, such as Pr^{3+} [29]. The interesting phenomenon of metal cations such as Pr^{3+} entering into channels and the inner capsule, thereby constituting a novel situation with a metal center in two different environments corresponding to a coordination chemistry under confined conditions or, in other words, cation transfer in a controlled and specific fashion, has been reported. The reported findings open up perspectives for a special type of en capsulation chemistry, i.e. coordination chemistry under confined conditions. This can be extended to (1) a variety of ligands like the present one, (2) different capsule charges, (3) different types of porosity, (4) different solvent molecules like water and (5) different metal centers. In addition, the presence of cations such as Pr^{3+} in two different coordination geometries gives a unique opportunity to study the ligand influence on the electronic structure of rare earth compounds.

Furthermore, nanocapsules have given us also the opportunity to study the structures of the simplest chemical reagent we have in our hands, namely pure H_2O. Even though it is the simplest chemically known compound, it gives rise to a plethora of structural motifs which are difficult to study [30]. The use of nanocapsules as "crystallization flasks" has given the advantage of isolating different kinds of water structures, while the same system can also be studied as a probe to investigate "complex system" behavior in general, and further, a "new state of inorganic ions" involved in the formation of a novel type of aggregates [31], even allowing the control of the aggregate size by the change in the cluster charge. It is even possible to incorporate large cluster guests, e.g. $\{PMo_{12}O_{40}\}^{3-}$, within the Fe-substituted Keplerate cluster $\{Mo_{72}Fe_{30}\}$, where the Keplerate host acts rather like a prison, totally encompassing the guest or, more precisely, a hostage molecule to give
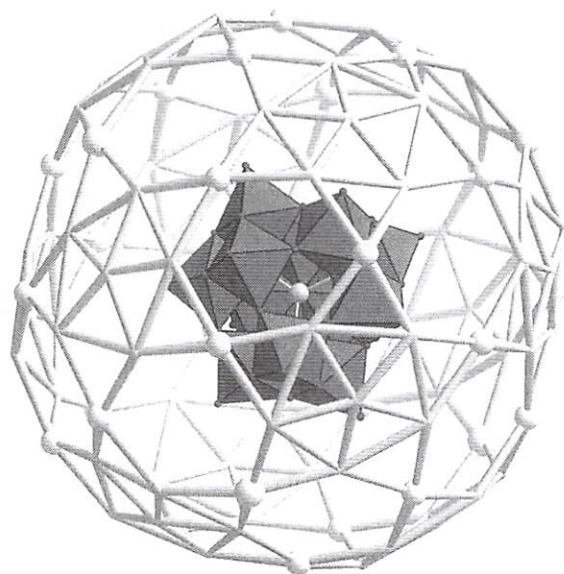
Figure 11.8 (a) Structure of $\{Mo_{12}\} \subset [\{Mo_{132}\}$. The hostage is shown in polyhedral form and the $\{Mo_{72}Fe_{30}\}$ is shown as the framework with the $\{Fe\}$ positions shown as white spheres linking the 12 $\{(Mo^{VI})Mo^{VI}_5\}$ pentagons, and the Keggin nucleus in polyhedral representation.

the compound $[PMo_{12}O_{40\{(Mo^{VI})}Mo^{VI}_5\}_{12}Fe^{III}O_{252}(H_2O)_{102}(CH_3COO)_{15}].\sim 120 H_2O$ (Figure 11.8) [32,33].

11.6
Surface-Encapsulated Clusters (SECs): Organic Nanostructures with Inorganic Cores

In an effort to combine inorganic polyoxometalates and organic materials chemistry, cationic surfactants have been applied to improve the surface properties of POMs. The resulting surfactant-encapsulated complexes (SECs) are compatible with organic matrixes, improve the stability of the encapsulated cluster against fragmentation, enhance the solubility in nonpolar, aprotic organic solvents and neutralize their charge, thus leading to discrete, electrostatically neutral assemblies, while altering the surface chemical properties in a predictable manner. Importantly, the basic physical and chemical properties of the polyoxometalates are retained [34] while the coexistence of hydrophobic alkyl chains and hydrophilic clusters in SECs gives them an amphiphilic character. Recently, it has been reported that this amphiphilic character is also exhibited in a solution environment and an unusual vesicular assembly of $(DODA)_4H$ $[Eu(H_2O)_2SiW_{11}O_{39}]$ $(DODA =$ dimethyldioctadecylammonium) has been observed [35]. An even larger aggregation

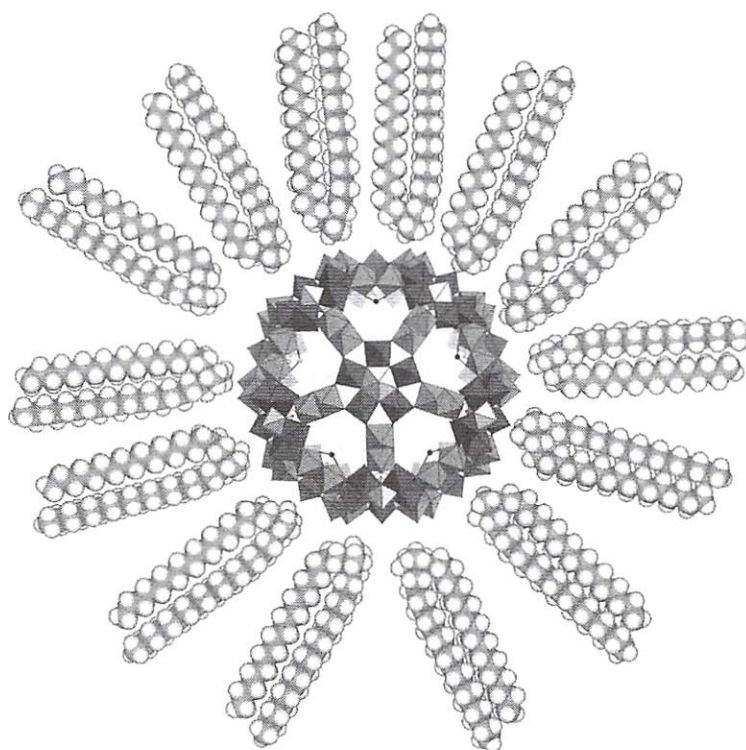**Figure 11.9** {Mo_{132}} SEC cluster $(DODA)_{40}(NH_4)_2 [(H_2O)_n Mo_{132}O_{372}(CH_3CO_2)_{30} (H_2O)_{72}]$ showing the inorganic core and the "soft" organic outer shell.

has been reported recently, the "onion"-like structure $(DODA)_4SiW_{12}O_{40}$ [36] and $(DODA)_{40}(NH_4)_2 [(H_2O)_n Mo_{132}O_{372}(CH_3CO_2)_{30} (H_2O)_{72}]$ [37,38] (Figure 11.9) and also $(DODA)_{20}(NH_4) [H_3Mo_{57}V_6(NO)_6O_{183}(H_2O)_{18}]$ [39], where the spherical species can provide a similar microenvironment to vesicles, which makes these assemblies suitable carriers to perform the catalytic and pharmacological functions of polyoxometalates. Moreover, the ability of polyoxometalates to undergo multiple reduction/oxidation steps may be exploited in information storage devices or optical switches. The possibility of fabricating well-defined two-dimensional arrays is an important step towards this goal.

The above-mentioned findings and suggestions reveal the feasibility of utilizing SECs as polyoxometalate-containing amphiphiles to construct regular assemblies from solution, help us to comprehend the catalyzing reactions of polyoxometalates in organic media, promote the effective interaction with organic molecules of biological interest and enhance, potentially, the interaction with biological media. However, the origin of the assembly process and whether it is a general behavior of SECs in solution are both still the subject of much debate and study.

11.7
Perspectives

It is clear that polyoxometalate-based building blocks can provide routes to the designed assembly of nanoscale capsules using coordinative interactions. This in turn is leading to and defining new areas of chemistry, i.e. under confined conditions, with parallels to processes/situations in biological cells regarding cell response and ion transport and even the possibility of engineering systems which exhibit complex and maybe adaptive behavior allowing chemical emergence. One tantalizing objective is the observation of evolving and dissipative inorganic systems. Generally, matter can be studied under confined conditions while the discovery of new systems resulting from encapsulation reveals new phenomena not observable in the bulk. This includes "confined water" with and without electrolytes and also spectacular chemical reactions. The presence of well-defined cavities/nanospaces and gated pores allows specific interactions of the capsules with their environments and subsequent uptake and selective binding of guests, since the architectures of the inner cluster walls can be "programmed/redesigned". Therefore, the design and synthetic approaches to polyoxometalates and the fact that these clusters can be constructed over multiple length scales, along with their almost unmatched range of physical properties, mean that they are serious candidates to be used as the functional part of any nano-device. The challenge now is to design individual POM cluster molecules that can interact both with each other and with the macroscale, in a desired fashion in response to inputs and environmental effects, so a functioning molecular system is really constructed. These capsule systems are truly fascinating and the future is exciting, since great leaps in understanding the principles that underpin the assembly mechanisms of such capsules allow the designed construction of extremely complex and specifically interacting systems – and this in the broadest sense is "bringing inorganic chemistry to life".

References

1 Sato, S., Iida, J., Suzuko, K., Kawano, M., Ozeki, T. and Fujita, M. (2006) *Science*, 313, 1273.

2 Müller, A., Beckmann, E., Bögge, H., Schmidtmann, M. and Dress, A. (2002) *Angew. Chem. Int. Ed.*, 41, 1162.

3 Pope M.T. and Muller A. (eds) (2001) *Polyoxometalate Chemistry: from Topology via Self-Assembly to Applications*, Kluwer, Dordrecht. Wassermann, K., Dickman, M.H. and Pope, M.T. (1997) *Angew. Chem. Int. Ed. Engl.*, 36, 1445.

4 Long, D.-L., Burkholder, E. and Cronin, L. (2007) *Chem. Soc. Rev.*, 36, 105.

5 Cronin, L. (2004) in *Comprehensive Coordination Chemistry II*, (eds J.A. McCleverty and T.J. Meyer), Vol. 7 Elsevier, Amsterdam, pp. 1–56.

6 Neumann, R. and Dahan, M. (1997) *Nature*, 388, 353; Mizuno, N. and Misono, M. (1998) *Chem. Rev.*, 98, 199.

7 Katsoulis, D.E. (1998) *Chem. Rev.*, 98, 359; Yamase, T. (1998) *Chem. Rev.*, 98, 307.

8 Rüther, T., Hultgren, V.M., Timko, B.P., Bond, A.M., Jackson, W.R. and Wedd, A.G. (2003) *J. Am. Chem. Soc.*, **125**, 10133.

9 Long, D.L., Kogerler, P., Parenty, A.D.C., Fielden, J. and Cronin, L. (2006) *Angew. Chem. Int. Ed.*, **45**, 4798.

10 Scheele, C.W. (1971) in *Sämtliche Physische und Chemische Werke*, (ed. D.S.F. Hermbstädt), M. Sändig, Niederwalluf/Wiesbaden, Vol. 1 pp. 185–200 (reprint; original published 1783).

11 Müller, A., Krickemeyer, E., Meyer, J., Bögge, H., Peters, F., Plass, W., Diemann, E., Dillinger, S., Nonnenbruch, F., Randerath, M. and Menke, C. (1995) *Angew. Chem. Int. Ed.*, **34**, 2122.

12 Cronin, L., Diemann, E. and Müller, A. (2003) in: *Inorganic Experiments*, (ed. Woollins J.D.), Wiley-VCH, Weinheim, pp. 340–346.

13 Cronin, L., Beugholt, C., Krickemeyer, E., Schmidtmann, M., Bögge, H., Kögerler, P., Luong, T.K.K. and Müller, A. (2002) *Angew. Chem. Int. Ed.*, **41**, 2805.

14 Müller, A., Das, S.K., Talismanov, S., Roy, S., Beckmann, E., Bögge, H., Schmidtmann, M., Merca, A., Berkle, A., Allouche, L., Zhou, Y.S. and Zhang, L.J. (2003) *Angew. Chem. Int. Ed.*, **42**, 5039.

15 Long, D., Abbas, H., Kogerler, P. and Cronin, L. (2004) *Angew. Chem. Int. Ed.*, **43**, 1817.

16 Long, D., Abbas, H., Kogerler, P. and Cronin, L. (2005) *Angew. Chem. Int. Ed.*, **44**, 3415.

17 Long, D., Abbas, H., Kögerler, P. and Cronin, L. (2004) *J. Am. Chem. Soc.*, **126**, 13880.

18 Long, D.L., Brucher, O., Streb, C. and Cronin, L. (2006) *Dalton Trans.*, 2852.

19 Müller, A., Kögerler, P. and Bögge, H. (2000) *Struct. Bonding*, **96**, 203.

20 Müller, A., Krickemeyer, E., Bögge, H., Schmidtmann, M. and Peters, F. (1998) *Angew. Chem. Int. Ed.*, **37**, 3359.

21 Müller, A., Krickemeyer, E., Bögge, H., Schmidtmann, M., Botar, B. and Talismanova, M.O. (2003) *Angew. Chem. Int. Ed.*, **42**, 2085.

22 Müller, A., Krickemeyer, E., Bögge, H., Schmidtmann, M., Roy, S. and Berkle, A. (2002) *Angew. Chem. Int. Ed.*, **41**, 3604.

23 Müller, A., Botar, B., Bögge, H., Kögerler, P. and Berkle, A. (2002) *Chem. Commun.*, 2944.

24 Müller, A., Das, S.K., Talismanov, S., Roy, S., Beckmann, E., Bögge, H., Schmidtmann, M., Merca, A., Berkle, A., Allouche, L., Zhou, Y.S. and Zhang, L.J. (2003) *Angew. Chem. Int. Ed.*, **42**, 5039.

25 Müller, A., Rehder, D., Haupt, E.T.K., Merca, A., Bögge, H., Schmidtmann, M. and Heinze-Brückner, G. (2004) *Angew. Chem. Int. Ed.*, **43**, 4466.

26 Haupt, E.T.K., Wontorra, C., Rehder, D., Müller, A. (2005) *Chem. Commun.*, 3912. Müller, A., Botar, B., Bögge, H., Kögerler, P. and Berkle, A. (2002) *Chem. Commun.*, 2944.

27 Müller, A., Toma, L., Bögge, H., Schäffer, C. and Stammler, A. (2005) *Angew. Chem. Int. Ed.*, **44**, 7757.

28 Müller, A., Zhou, Y., Bögge, H., Schmidtmann, M., Mitra, T., Haupt, E.T.K. and Berkle, A. (2006) *Angew. Chem. Int. Ed.*, **45**, 460.

29 Müller, A., Zhoua, Y., Zhang, L., Bogge, H., Schmidtmann, M., Dresselb, M. and van Slageren, J. (2004) *Chem. Commun.*, 2038.

30 Müller, A., Krickemeyer, E., Bogge, H., Schmidtmann, M., Botar, B. and Talismanova, M.O. (2003) *Angew. Chem. Int. Ed.*, **42**, 2085.

31 Müller, A., Diemann, E., Kuhlmann, C., Eimer, W., Serain, C., Tak, T., Knoechel, A. and Pranzas, P.K. (2001) *Chem. Commun.*, 1928.

32 Müller, A., Das, S.K., Kögerler, P., Bögge, H., Schmidtmann, M., Trautwein, A.X., Schünemann, V., Krickemeyer, E. and Preetz, W. (2000) *Angew. Chem. Int. Ed.*, **112**, 3556.

33 Müller, A., Todea, A.M., Bogge, H., van Slageren, J., Dressel, M., Stammlera, A. and Rusuc, M. (2006) *Chem. Commun.*, 3066.

34 Tao, Y., Yu, Q. and Bu, X.H. (2007) *Chem. Commun.*, **15**, 1527.

35 Li, J.R., Bu, W., Li, H., Sun, H., Yin, S. and Wu, L. (2005) *J. Am. Chem. Soc.*, **127**, 8016.

36 Li, H., Sun, H., Qi, W., Xu, M. and Wu, L. (2007) *Angew. Chem. Int. Ed.*, **46**, 1300.

37 Kurth, D.G., Lehmann, P., Volkmer, D., Müller, A. and Schwahn, D. (2000) *J. Chem. Soc., Dalton Trans.*, 3989.

38 Kurth, D.G., Lehmann, P., Volkmer, D., Cölfen, H., Koop, M.J., Müller, A. and Chesne, A.D. (2000) *Chem. Eur. J.*, **6**, 385.

39 Volkmer, D., Chesne, A.D., Kurth, D.G., Schnablegger, H., Lehmann, P., Koop, M.J. and Müller, A. (1995) *J. Am. Chem. Soc.*, **46**, 122.